V2V Channels and Performance of Multiuser Spread Spectrum Modulation

Indranil Sen and David W. Matolak, Ohio University

Abstract: *Vehicle-to-vehicle (V2V) communications have drawn much attention in recent years. In this article, we discuss tradeoffs between implementation complexity and accuracy of several stochastic channel models for the V2V environment, and then address spread-spectrum system performance attained using these channel models. Two different propagation environments are considered: urban and open areas (highways). The necessity of employing nonstationary channel models to accurately represent the channel is substantiated by comparing stationary and nonstationary empirical model outputs with measured data. A framework to compare single-carrier direct sequence code division multiple access (SC-DS-CDMA) and multicarrier DS-CDMA (MC-DS-CDMA) performance in V2V channels is presented, and bit error ratio (BER) performance of the schemes is provided for the two channels. Our comparison of single- and multi-user performance shows that MC-DS-CDMA performs better than SC-DS-CDMA in both V2V environments.*

Vehicle-to-vehicle (V2V) communications will constitute an integral part of future intelligent transportation systems (ITSs) [1]. Recognition of this has initiated a growing amount of recent work on various aspects of ITS [2]. The consumer aim of being connected everywhere implies an eventual need for V2V connectivity. Various civil applications are also envisioned. Some of the obvious benefits of such communication capabilities are enhanced commuter awareness of traffic conditions and improved road safety, faster processing at toll booths, and a flow of multimedia content among different traveling cars.

A recent standard for V2V communication in the 5.9-GHz unlicensed national information infrastructure (UNII) band has been developed [1]. This standard aims to support high-mobility platforms using the

Digital Object Identifier 10.1109/MVT.2008.917453

 1556-6072/07/$25.00©2007IEEE

V2V COMMUNICATIONS WILL COMPOSE AN INTEGRAL PART OF FUTURE INTELLIGENT TRANSPORTATION SYSTEMS.

802.11protocol [3]. Reference [4] proposes a prototype wireless transmission system for transmitting multimedia information at a maximum rate of 4.608 Mb/s in the 5.2-GHz frequency band. This system is based on a spread-spectrum multicode transmission scheme that uses cyclic shifted-and-extended m sequences, and is designed for ITS applications. In [4], the V2V channels considered were additive white Gaussian noise (AWGN), single-path Rayleigh fading, and two-tap Rayleigh fading with equal power in both channel taps. These channel models, while convenient for analysis and simulation, are much simpler than the actual channel that will be encountered in practice. To ensure reliable system performance, it is necessary to evaluate systems using realistic channel models before deployment. This is the intent of this article.

We have developed stochastic channel models for various V2V communication settings using measured data [5]. We use these models to evaluate performance of some newer multicarrier transmission schemes. Recently, a considerable amount of research, e.g., [6]–[8], has been done to evaluate the performance of these schemes in the presence of multipath fading. The research presented in this article is an effort to extend these multicarrier results by evaluating single- and multicarrier direct sequence spread-spectrum system performance in V2V fading channels.

System and Channel Description

System Description

We address two systems here: single-carrier direct sequence code division multiple access (DS-CDMA), or SC-DS-CDMA, and multicarrier DS-CDMA (MC-DS-CDMA). The transmitter block diagram for MC-DS-CDMA systems is similar to those in [6]. The carrier frequency for subcarrier i is $f_{c,i} = f_c + i/T_{c,MC}$; hence, there is partial overlap among the spectra of neighboring subcarriers. Without loss of generality and for ease of analysis, binary phase shift keying (BPSK) is used on each subcarrier. We replicate the bits on each subcarrier to provide frequency diversity. The transmitted MC-DS signal for user k, $s^{(k)}(t)$, is

$$s^{(k)}(t) = \sum_{i=1}^{M} A_i d^{(k)}(t) c_i^{(k)}(t) \cos(2\pi f_i t), \qquad (1)$$

where $A_i = \sqrt{2E_b/M^2T_b}$; E_b and T_b are the bit energy and duration, respectively; and M is the number of subcarriers. The data waveform $d^{(k)}(t)$ and spreading waveform $c_i^{(k)}(t)$ are

$$d^{(k)}(t) = \sum_n d^{(k)}(n) p_{T_b}(t - nT_b),$$

$$c_i^{(k)}(t) = \sum_{m=0}^{N_{MC}-1} c_i^{(k)}(m) p_{T_{c,MC}}(t - mT_{c,MC}), \qquad (2)$$

where $d^{(k)}(n) \in \{\pm 1\}$ is the kth users' nth data bit and $c_i^{(k)}(m) \in \{\pm 1\}$ is the mth chip of the kth users' spreading code. The MC-DS-CDMA processing gain is $N_{MC} = T_b/T_{c,MC}$ and $p_{T_{c,MC}}$ is the rectangular pulse waveform. The transmitter for SC-DS-CDMA can be derived from (1) by setting $M = 1$. For a fair comparison between the two systems, we equate the number of users K, the per user data rate (R_b), and the bandwidth (10 MHz) available for each system. The bandwidth for SC-DS-CDMA and MC-DS-CDMA is approximately $2R_bN_{SC}$ and $(M+1)R_bN_{MC}$, respectively. In this article, we configure the systems as follows: the number of subcarriers used for MC-DS-CDMA is three and the data rates considered are 160 and 80 kb/s. For $R_b = 160$ kb/s, $N_{SC} = 32$ and $N_{MC} = 16$. Similarly, for $R_b = 80$ kb/s, $N_{SC} = 64$ and $N_{MC} = 32$. The bandwidth for SC-DS-CDMA is 10 MHz and each subcarrier of MS-DS-CDMA has a bandwidth of 5 MHz.

Channel Descriptions

The physical channel can be modeled as a time-varying linear filter. The most commonly used model for the channel is the tapped-delay line model [9]. The channel impulse response (CIR) for user k is

$$h^{(k)}(t) = \sum_{i=0}^{L-1} z_i^{(k)}(t) \alpha_i^{(k)}(t) e^{j\phi_{i,k}(t)} \delta(t - \tau_i)$$

$$= \sum_{i=0}^{L-1} h_i^{(k)} e^{j\phi_{i,k}(t)} \delta(t - \tau_i), \qquad (3)$$

where the τs are delays, the αs are the random amplitudes, the ϕs are the random aggregate phases, and the zs $\in \{0, 1\}$ are random on-off switching processes that model the appearance and disappearance of multipath components. For modeling amplitudes, we use the Weibull distribution, which is a generalized fading distribution similar to the Nakagami-m distribution. The Weibull probability density function (pdf) is $f_W(w) = (\beta/\gamma^\beta) w^{(\beta-1)} \exp(-w^\beta/\gamma^\beta)$, where $\beta > 0$ is the fading parameter, which indicates the severity of fading. Parameter γ is related to the average power Ω given by $\Omega = E[w^2] = \gamma^2\Gamma[1 + (2/\beta)]$ with Γ the gamma function. The number of taps in the model is L. The persistence process $z(t)$ is used to account for the

finite lifetime of the propagation paths and is modeled using a two-state first-order Markov chain. State 1 denotes the presence of multipath in a given delay bin and state 0 signifies the absence of multipath. The Markov model is specified by two matrices, the transition (*TS*) matrix and the steady-state (*SS*) matrix:

$$TS = \begin{bmatrix} P_{00} & P_{01} \\ P_{10} & P_{11} \end{bmatrix}, \qquad SS = \begin{bmatrix} P_0 \\ P_1 \end{bmatrix}. \tag{4}$$

Each element P_{ij} in matrix *TS* is defined as the probability of going from state i to state j, and each SS element P_j gives the steady-state probability associated with the jth state.

We obtain L via the maximum RMS delay spread $\sigma_{\tau,max}$,

$$L = |\sigma_{\tau,\max}/T_c| + 1, \tag{5}$$

where T_c is the chip duration. For brevity, in this article, we limit our focus to two regions, urban, antenna outside car (UOC) and highway, open, high traffic density (OHT) [5]. To allow a tradeoff between implementation complexity and model accuracy, we propose three different channel models for each region.

- Model 1: In this model, L is truncated to account for 99% of the energy. For example, for UOC, $\sigma_{\tau,max}$ is 1,328 ns, so L is 15 for a 10-MHz bandwidth. But since we can gather 99% of the energy with the first four taps, we significantly reduce model complexity by using only the first four taps. We have also found that the tap amplitudes are correlated. Detailed channel models, with amplitude statistics and correlation coefficient matrices for Model 1, for different regions are provided in [5].
- Model 2: For this model, we don't truncate L. Considering the same example as in Model 1, for a 10-MHz UOC channel, Model 2 has 15 taps.
- Model 3: In this model, the number of taps is the same as in Model 2, but we use the wide sense stationary, uncorrelated scattering (WSSUS) approximation [10]. As is well known, the WSSUS approximation is often used to reduce channel model complexity. Our intent in introducing Model 3 is to compare WSSUS and non-(WSSUS) implementations of the same channel with the actual channel data; thus Model 3 does not use correlation or the persistence processes.

A RECENT STANDARD FOR V2V COMMUNICATION IN THE 5.9-GHZ UNII BAND HAS BEEN DEVELOPED.

Table 1 compares the RMS delay spread (RMS-DS) and delay window (DW) statistics of the CIRs generated using the different models with those of the measured data. The delay window ($W_{\tau,x}$) is defined as the length of the middle portion of the CIR containing x% of the total CIR energy. For most cases, $W_{\tau,x}$ can be interpreted in the same manner as σ_τ: the larger the value of $W_{\tau,x}$, the more dispersive the channel [11]. For comparison, we have considered 10-MHz OHT models; similar results for UOC appear in [5]. To compare the shapes of the pdfs for $W_{\tau,90}$ and σ_τ, we also provide statistics that are used to measure distance of a true distribution (here, the measured data, denoted D) to that of the simulated model (denoted S). The two distance measures we use are the Kullback-Leibler (KL) [12] and histogram intersection (HI) [13]. Consider S_i and D_i as the set of probability density values for the two pdfs; then the following are the definitions for the distances:

$$KL = \sum_{i=1}^{M} D_i \log_2\left(\frac{D_i}{S_i}\right),$$
$$HI = \sum_{i=1}^{M} \min(D_i, S_i), \tag{6}$$

where M is the number of points in the pdf domain. From (6), we can state that if the pdfs are identical, then

TABLE 1 *Comparison of statistics of Model 1, Model 2, and Model 3 with those of data for 10-MHz OHT regions.*

Parameter	Data	Model 1	Model 2	Model 3
		Statistics [min; mean; max] (ns)		
RMS-DS	[0.5 126.8 1,773]	[0 23.3 95.3]	[0 109 847]	[0 185.4 732.7]
DW-90	[100 233.4 4,100]	[100 104.4 200]	[100 252 1,800]	[200 355.8 2,600]
		Distance with respect to pdf of collected data		
KL-RMS-DS	0	0.7429	0.0276	0.3664
HI-RMS-DS	1	0.5325	0.8579	0.5729
KL-DW-90	0	0.1666	0.0137	2.0496
HI-DW-90	1	0.7953	0.8781	0.1987

KL should be zero and *HI* should be one. From Table 1, we can conclude that Model 2 provides the most faithful representation of the actual data for OHT channels. Model 3 provides a pessimistic channel representation. This illustrates the need for nonstationary correlated channel models to accurately model the propagation channel. Table 2 provides the tap amplitude statistics and persistence process parameters for Model 2, 10 MHz, OHT. A similar comparison of different models for UOC is provided in [5]; 10-MHz UOC Model 1 and Model 2 parameters are also provided in [5].

TABLE 2 *Channel fading amplitude and persistence parameters, [Model-2, 10 MHz, OHT].*

Tap Index k	Energy	β_k	P_1	$P_{00,k}$	$P_{11,k}$
1	0.8982	4.3000	1.0000	na	1.0000
2	0.0527	1.6055	0.7960	0.3625	0.8366
3	0.0159	1.8462	0.5696	0.5999	0.6973
4	0.0084	1.8530	0.3739	0.7325	0.5514
5	0.0064	1.7160	0.2764	0.8121	0.5084
6	0.0042	1.6659	0.1976	0.8641	0.4486
7	0.0027	1.7037	0.1444	0.9037	0.4297
8	0.0026	1.8428	0.1178	0.9222	0.4172
9	0.0018	1.7886	0.0856	0.9414	0.3750
10	0.0010	2.0063	0.0576	0.9592	0.3333
11	0.0012	1.9870	0.0598	0.9544	0.2844
12	0.0010	1.9168	0.0467	0.9640	0.2647
13	0.0006	2.1577	0.0404	0.9694	0.2721
14	0.0008	2.0626	0.0296	0.9759	0.2130
15	0.0006	2.5831	0.0362	0.9729	0.2803
16	0.0003	2.2830	0.0285	0.9794	0.2981
17	0.0006	2.3446	0.0264	0.9808	0.2917
18	0.0005	2.6841	0.0206	0.9829	0.1867
19	0.0005	2.4252	0.0178	0.9869	0.2769

Analysis

In this section, we provide analysis of synchronous SC-DS-CDMA using Model 3; analysis for the other schemes is omitted for brevity. The received signal is given by

$$r(t)=\sum_{k=1}^{K}\sum_{l=0}^{L-1}\left[h_l^{(k)}\sqrt{\tfrac{2E_b}{T_b}}d^{(i)}\left(t-\tau_l^{(k)}\right)c^{(i)}\left(t-\tau_l^{(k)}\right)\cos\left(2\pi f_c t-\theta_l^{(k)}\right)\right]+n(t), \tag{7}$$

where $\theta_l^{(k)}=2\pi f_c\tau_l^{(l)}+\phi_{l,k}$ are independent, identically distributed random variables (i.i.d. rvs) uniformly distributed in $[0,2\pi)$ and $n(t)$ is AWGN with double-sided PSD of $N_0/2$ W/Hz. The receiver is a conventional RAKE receiver. The decision statistic of the kth user is

$$Z^{(k)}=\sum_{m=0}^{L-1}Z_m^{(k)}, \tag{8}$$

where we let $\tau_l=0$ for notational brevity. The correlator output for the mth tap for user k is

$$Z_m^{(k)}=\int_0^{T_b}r(t)h_m^{(k)}c^{(k)}(t)\cos\left(2\pi ft-\theta_l^{(k)}\right)dt. \tag{9}$$

Since only relative delay is of interest in the analysis, the delay is set to be zero for the first tap of user k, and the delay of the other taps of different users are referenced to this.

The correlator output can be separated into four terms, i.e., $Z_m^{(k)}=D+I+ICI+MAI$, where the desired signal term is

$$D=h_m^{(k)^2}\sqrt{E_bT_b/2},$$

I is the zero-mean AWGN term with variance $h_m^{(k)^2}N_0T_b/4$, *ICI* is the inter-chip interference from the same user, and MAI is multiple access interference from different users. The ICI is given by

$$ICI=\sum_{\substack{l=0\\l\neq m}}^{L-1}h_l^{(k)}h_m^{(k)}\cos\left[\phi_{(l,m)}^{(k,k)}\right]\times\sqrt{\frac{E_b}{2T_b}}\int_0^{T_b}d^{(k)}(t-lT_c)c_i^{(k)}(t-lT_c)c^{(k)}(t)dt,$$

with $\phi_{(l,m)}^{(k,k)}=\theta_l^{(k)}-\theta_m^{(k)}$ uniformly distributed in $[0,2\pi)$. The integral in the zero-mean ICI term is

$$\int_0^{T_b}d^{(i)}(t-lT_c)c_i^{(i)}(t-lT_c)c^{(i)}(t)dt=d^{(i)}(-1)T_c\sum_{j=0}^{l}c^{(i)}(m)c^{(i)}(m-l)+d^{(i)}(0)T_c\times\sum_{j=l+1}^{N-1}c^{(i)}(m)c^{(i)}(m-l).$$

Since the spreading codes used are combined Walsh and random long codes, $c(m)c(m-l)=\pm1$ equiprobably. The ICI variance is then

$$\text{var}[\,ICI\,] = \sum_{\substack{l=0 \\ l\neq m}}^{L-1} \text{var}[\,I_{1,l}\,]$$

$$= \sum_{\substack{l=0 \\ l\neq m}}^{L-1} \Omega_l^{(k)} \left[h_m^{(k)}\right]^2 \frac{E_b T_b}{4N}. \qquad (10)$$

We can do a similar analysis for the zero-mean MAI

$$MAI = \sum_{\substack{K=1 \\ K\neq i}}^{K} \sum_{\substack{l=0 \\ l\neq m}}^{L-1} \times \left[h_l^{(k)} h_m^{(i)} \cos\left[\phi_{(l,m)}^{(k,i)}\right] \sqrt{\frac{E_b}{2T_b}} \int_0^{T_b} d^{(k)}(t - lT_c) c^{(k)}(t - lT_c) c^{(i)}(t) dt \right]. \qquad (11)$$

Note that since we use orthogonal codes, the interference on user ks mth tap is zero. Hence, the variance of MAI is

$$\text{var}[MAI] = (K-1) \sum_{\substack{l=0 \\ l\neq m}}^{L-1} \Omega_l \left[h_m^{(k)}\right]^2 \frac{E_b T_b}{4N}. \qquad (12)$$

Thus, the bit error ratio (BER conditioned on the fading amplitude is

$$P_{b,SC}^{(k)}(\gamma_{SC}) = Q\left(\sqrt{2\gamma_{SC}}\right), \qquad (13)$$

with signal to noise plus inference ratio (SNIR) given by

$$\gamma_{SC} = \left\{ \frac{N_0}{E_b} + \frac{K(L-1)}{2NL} \right\}^{-1} \sum_{l=0}^{L-1} \left[h_l^{(k)}\right]^2.$$

The average BER is obtained by averaging the conditional $P_b^{(k)}$ over the joint pdf of the hs given by

$$\bar{P}_{b,SC}(\gamma) = \underbrace{\iiint \cdots \int}_{L-fold} Q\left(\sqrt{2\gamma_{SC}}\right) p_{h_1,h_2\ldots h_L}(\mathbf{h}) d\mathbf{h}. \qquad (14)$$

A similar analysis can also be done for the synchronous MC-DS-CDMA case, where the bits are replicated on each subcarrier. The SNIR for that case is

THE MOST COMMONLY USED MODEL FOR THE CHANNEL IS THE TAPPED-DELAY LINE MODEL.

$$\gamma_{MC} = \left[\sum_{i=1}^{M} \sum_{l=0}^{L-1} \left[h_{l,i}^{(k)}\right]^2 \right] \times \left\{ \frac{\frac{M^2 N_0}{E_b} + \frac{K(L-1)}{2NL}}{\sum_{i=1}^{M} \left[1 + \sum_{\substack{j=1 \\ j\neq i}}^{M} \sin c^2(\Delta f_{i,j} T_c) \right]} \right\}^{-1}. \qquad (15)$$

Numerical Results

In this section, we illustrate performance of SC-DS-SS and MC-DS-SS using simulations. (Analytical results assume independent taps and are, hence, slightly optimistic.) Since the BER performance of SC-DS and MC-DS is similar for M1 and M2, the M1 results are not presented for brevity. In Figure 1, we show single-user performance for

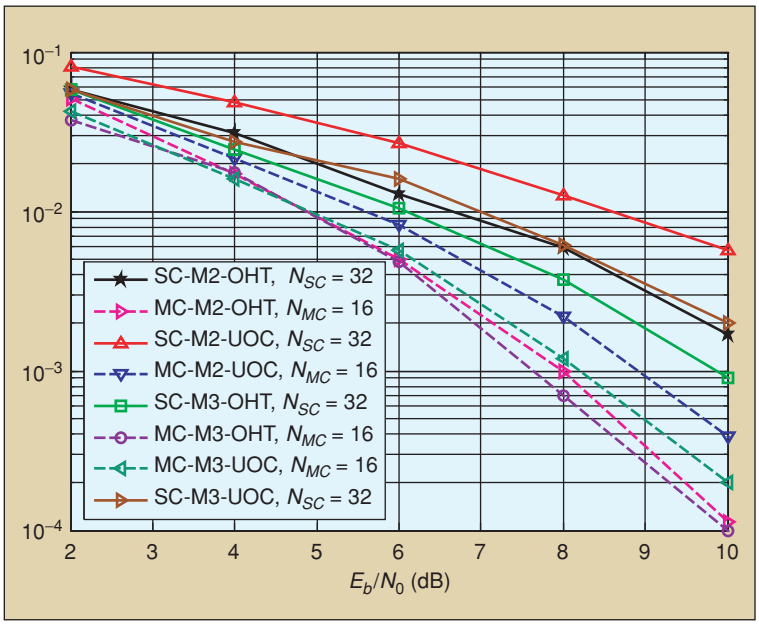

FIGURE 1 BER versus SNR using SC-DS and MC-DS ($M = 3$), Model 2 and Model 3, UOC and OHT, $K = 1$.

SC-DS ($N_{SC} = 32$) and MC-DS ($N_{MC} = 16$, $M = 3$) for the UOC and OHT channels. Both systems perform better in the OHT channel than in the UOC. This is expected since the UOC channel is more dispersive than the OHT. We assume ideal channel coefficient estimation in all simulations. For either region, performance of both modulations is worse on channel M2 than on M3. For a BER of

SINCE MC-DS PROVIDES FREQUENCY DIVERSITY IN ADDITION TO THE TIME DOMAIN PROCESSING GAIN, PERFORMANCE FOR ALL MODELS IS BETTER FOR MC-DS THAN IT IS FOR SC-DS.

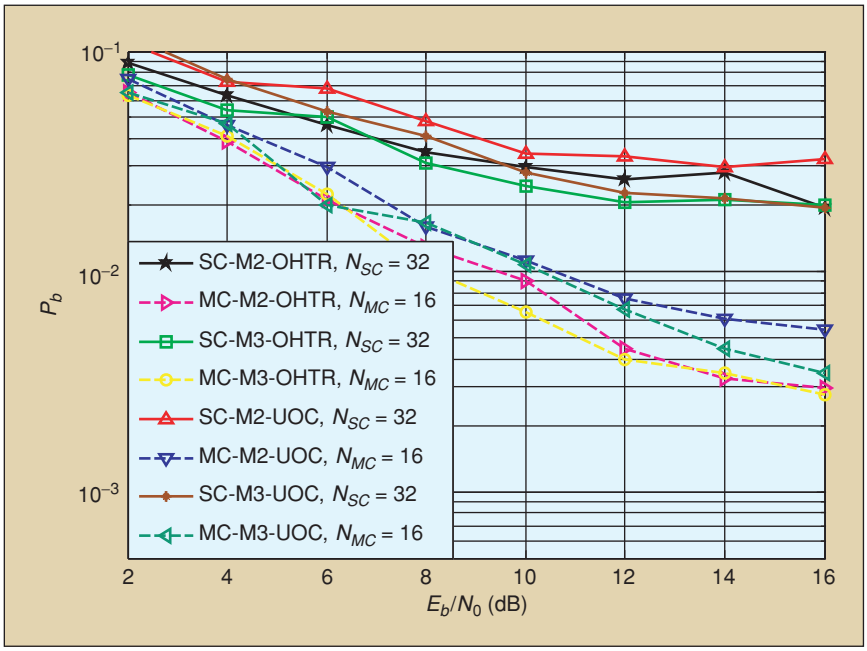

FIGURE 2 BER versus SNR using SC-DS and MC-DS ($M = 3$), Model 2 and Model 3, UOC and OHT, $K = 10$.

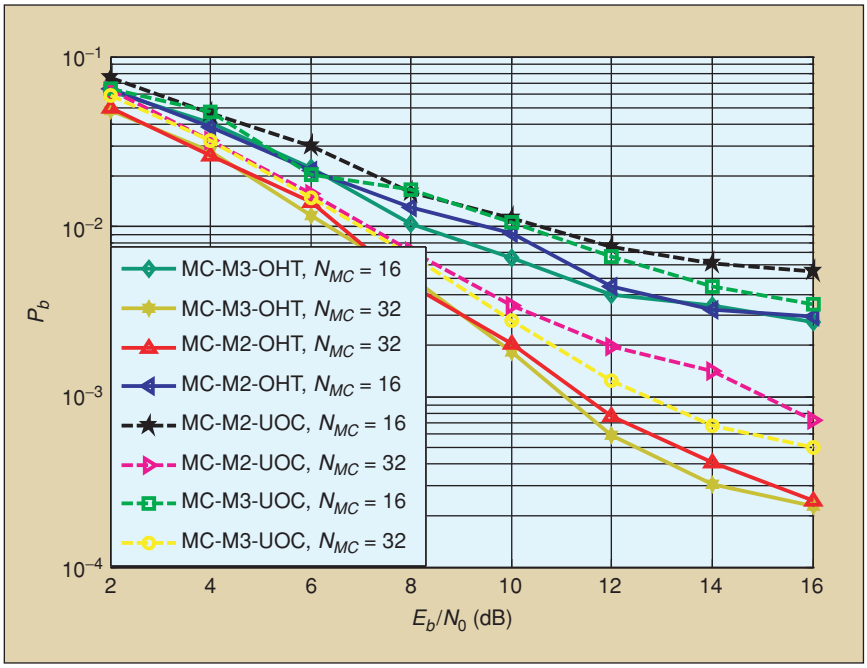

FIGURE 3 BER versus SNR using MC-DS ($M = 3$), Model 2 and Model 3, UOC and OHT, $K = 10$, $N_{MC} = 16, 32$.

$\sim 10^{-2}$, M2 requires ~1–1.5 dB more SNR than M3 for SC-DS and ~0.1–0.5 dB more than M3 for MC-DS. This slight gain in performance on M3 is due to the marginally higher frequency diversity provided by the more dispersive M3 channel. As discussed, since M2 is the more accurate model, results with M3 are optimistic. Figure 1 further supports our claim for the necessity of nonstationary correlated channel models (M2).

Also, since MC-DS provides frequency diversity in addition to the time domain processing gain, performance for all models is better for MC-DS than it is for SC-DS. Figure 2 illustrates performance of the spread-spectrum systems when there are ten users ($K = 10$). As expected, performance is much worse than in the single-user case due to MAI. In Figure 3, we compare MC-DS-CDMA performance for ten users for the different models using different values of processing gain N_{MC} (16, 32). Increasing processing gain improves performance on M2 significantly (e.g., at $P_b = 10^{-2}$ on M2, OHT gains ~2.5 dB and UOC gains around ~3.5 dB). On the other hand, with model M3 for both channels, performance gains of ~3 dB can be observed with larger processing gains. A similar comparison is provided for SC-DS for higher processing gains in Figure 4. The gains in performance for SC-DS using either model, in both regions, are less than those in Figure 3. Thus, we conclude that MC-DS-CDMA performs better than SC-DS-CDMA for both channels due to the presence of frequency and multipath diversity.

Conclusions

In this article, we discussed the tradeoff between implementation complexity and accuracy of several stochastic channel models for the V2V environment. We provided several ways of comparing the precision of the empirical channel models with respect to the measured data from which they were derived for two propagation regions: UOC and OHT. The need for nonstationary models

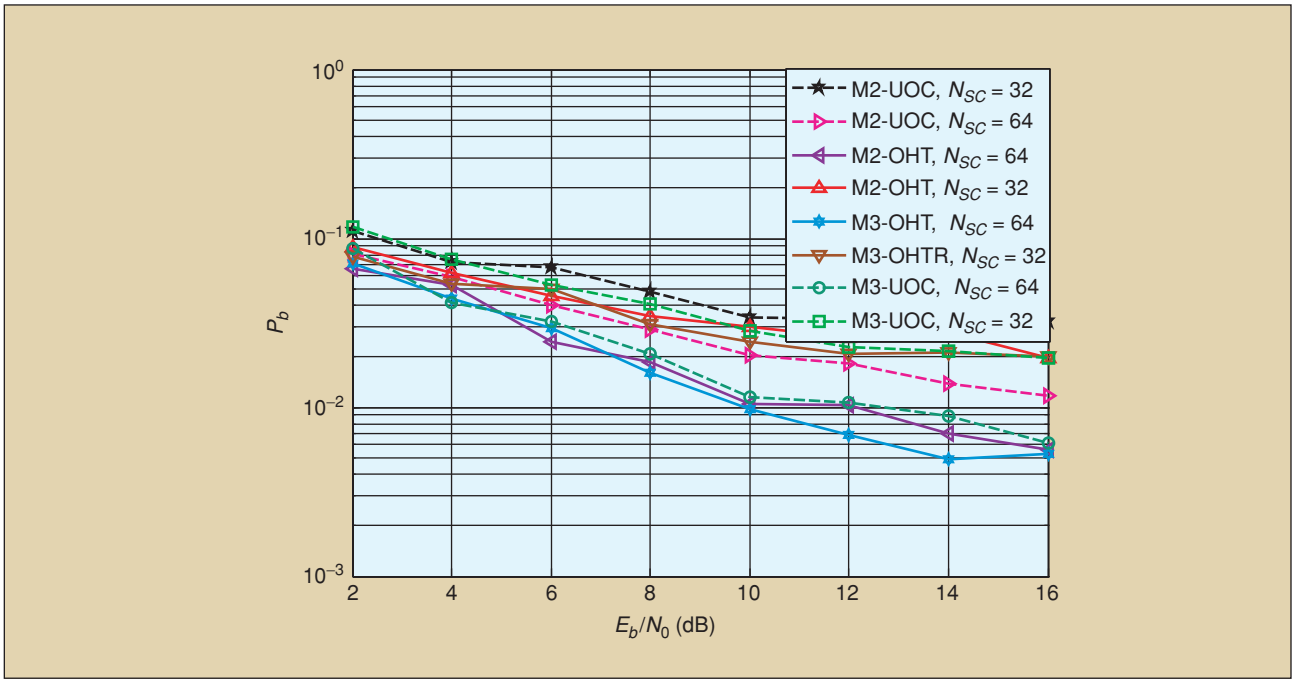

FIGURE 4 BER versus SNR using SC-DS, Model 2 and Model 3, UOC and OHT, $K = 10$.

to faithfully replicate actual propagation effects was discussed, and this was substantiated with experimental channel and analytical and simulated system performance results. We also described analysis results comparing SC-DS-CDMA and MC-DS-CDMA performance. BER performance of the modulation schemes for the different channels was presented. Single-user and multiuser performance was compared, and it was determined that MC-DS-CDMA performs the best in the given V2V environments.

Author Information

Indranil Sen received the B.E. degree from Mumbai University, India, in 2002, and the M.S. and Ph.D. degrees from Ohio University, Athens, in 2004 and 2007, respectively, both in electrical engineering. He is currently employed with the Corporate Technology Office of Motorola in Libertyville, Illinois. His areas of research interest are spread-spectrum communication, multicarrier waveform design, and channel modeling. He is a Student Member of the IEEE.

David W. Matolak received the B.S. degree from Pennsylvania State University in 1983, the M.S. degree from the University of Massachusetts in 1987, and the Ph.D. degree from the University of Virginia in 1995, all in electrical engineering. He worked at several communications companies (AT&T Bell Laboratories, MITRE, Lockheed Martin, L3 Communications) before joining Ohio University in 1999. His research interests are communication over fading channels, radio channel modeling, multicarrier transmission, and CDMA. He is a Senior Member of the IEEE and a member of Eta Kappa Nu and Sigma Xi. He has served on several IEEE conference technical program committees and was also chair of the Geo Mobile Radio Standards group in the TIA's Satellite Communications Division.

References

[1] *Standard Specification for Telecommunications and Information Exchange Between Roadside and Vehicle Systems—5GHz Band Dedicated Short Range Communications (DSRC) Medium Access Control (MAC) and Physical Layer (PHY) Specifications*, ASTM E2213, 2007.

[2] ITS project Web site [Online]. Available: http://www.its.dot.gov/index.htm

[3] *Wireless LAN Medium Access Control (MAC) and Physical layer (PHY) Specifications*, IEEE Std. 802.11, 1999.

[4] H. Harada and M. Fujise, "Feasibility study on a highly mobile microwave-band broad-band telecommunication system," *IEEE Trans. Intell. Transport. Systems*, vol. 3, no. 1, pp. 75–88, Mar. 2002.

[5] I. Sen and D.W. Matolak, "Vehicle to vehicle channel models for the 5 GHz band," submitted for publication.

[6] S. Kondo and L.B. Milstein, "Performance of multicarrier DS CDMA systems," *IEEE Trans. Comm.*, vol. 44, no. 2, pp. 238–246, Feb. 1996.

[7] E.A. Sourour and M. Nakagawa, "Performance of orthogonal multicarrier CDMA in a multipath fading channel," *IEEE Trans. Comm.*, vol. 44, pp. 356–366, Mar. 1996.

[8] L-L. Yang and L. Hanzo, "Performance of generalized multicarrier DS-CDMA over Nakagami-*m* fading channels," *IEEE Trans. Comm.*, vol. 50, no. 6, pp. 956-966, June 2002.

[9] J.G. Proakis, *Digital Communications*, 2nd ed. New York: McGraw-Hill, 1989.

[10] P. Bello, "Characterization of random time-variant linear channels," *IEEE Trans. Comm.*, vol. 11, pp. 360–393, Dec. 1963.

[11] *Multipath Propagation and Parameterization of its Characteristics*, ITU-R P.1407-1, 1999–2003.

[12] S. Kullback and R.A. Leibler, "On information and sufficiency," *Annals Math. Stat.* vol. 22, pp. 79–86, Jan. 1951.

[13] S. Boughorbely, J. Philippe Tarel, and N. Boujemaay, "Generalized histogram intersection kernel for image recognition," in *Proc. Int. Conf. Image Processing*, Genoa, IT, Sept. 2005, pp. 161-165. ***VT***